THE FLOW PULSATIONS IN A SYSTEM OF PARALLEL STEAM-GENERATING TUBES

V. B. Khabenskii and O. M. Baldina

UDC 621.1.01

A theoretical analysis is presented for the flow pulsations in a steam-generating pipe, which is based on computer integration of a system of equations in partial derivatives.

One cannot predict reasonably accurately the onset of pulsations in such a system because the process is complex and is affected by many parameters. Computer simulation is possible via a model for the nonstationary heat transfer and hydrodynamics, which involves a system of equations in partial derivatives for the conservation of energy, mass, and momentum in the homogeneous and two-phase flows [1], as well as the energy equation for the tube. There are numerous nonlinearities and the system is of high order, so the most precise numerical relationships are obtained by numerical computer integration. Special attention has been given to the form of the equations and the algebraic relationships that accompany the differential equations. The straight-line method has been used to solve the system of equations in partial derivatives. A fourth-order Runge–Kutta treatment was used to solve the resulting system of ordinary differential equations, which has major nonlinearities.

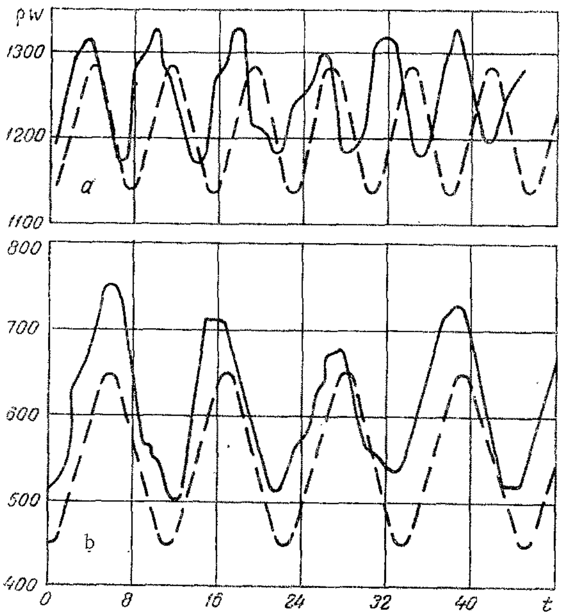

Fig. 1. Time variation in the mass flow rate at a tube inlet during pulsations (full line from measurement, broken line from calculation): a) conditions of run 28 [10] (q = 355 000 kcal /$m^2 \cdot h$: T_{in} = 264.9°C; P = 57.8 kg/cm^2); b) conditions of run 438 [10] (q = 191,500 kcal /$m^2 \cdot h$; T_{in} = 270.5°C; P = 100 kg/cm^2).

One has to make a careful choice of the coordinate system in which to represent the equations, because there are two media (homogeneous and two-phase), the heat flux varies along the tube, the two-phase mixture does not adhere to the wall, and the boundary between the two media shifts considerably during transients.

Lagrange or Euler coordinates may be used for the system of differential difference equations. If Lagrange coordinates are used, major difficulties arise if the medium does not adhere to the wall and the tube is unevenly heated [2]. The Euler system [3] is free from these deficiencies, but it is rational if the medium has a boundary between the phases whose position varies in time, since the system does not respond to the position of the boundary when this lies within a spatial element. Also, there is a discontinuity in the velocity when the boundary moves from one spatial element to another. The disadvantages of the Euler representation can be minimized if one substantially reduces the step in the spatial coordinate, though this may impose a reduction in the time step in order to avoid numerical instability in the solution, and this may result in an impermissible increase in the machine time needed.

A considerable saving in machine time is possible if a Lagrange-Euler system is used, with the economizer section in the Lagrange representation and the evaporator one in the Euler representation.

Polzunov Central Boiler and Turbine Institute, Leningrad. Translated from Inzhenerno-Fizicheskii Zhurnal, Vol. 17, No. 5, pp. 819-828, November, 1969. Original article submitted December 12, 1968.

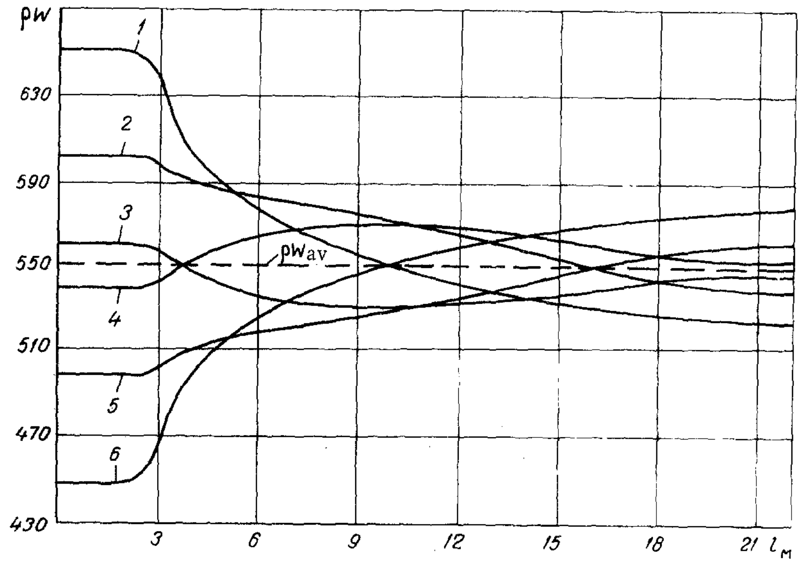

Fig. 2. Distribution of the mass flow rate along the tube length (m) during pulsations for times (sec) of: 1) 28, 2) 29.9, 3) 36.8, 4) 31.1, 5) 35.6, 6) 33.5.

The usual assumptions [2-5] were made in order to simplify the system, and these were shown to be justified for the parameters and perturbations characteristic of boilers.

The following form can then be given to the algebraic relationships and the system of equations.

1. The equations for the medium in element j in the economizer part:

$$\frac{dZ_j}{dt} = \frac{1}{2}\, w_{in} - \frac{4}{r_{in}}\, \frac{\alpha}{(\rho c_p)_{\bar{j}}}\, \frac{Z_j - Z_{j-1}}{T_j - T_{j-1}} \left[(T_q)_{\bar{j}} - \frac{1}{2}\,(T_j + T_{j-1}) \right] - \frac{dZ_{j-1}}{dt}\,, \tag{1}$$

where j = 0, 1, . . . k (k is the number of parts along the axis into which the economizer part is divided),

$$Z_{j=0} = 0;\quad Z_{j=k} = Z_{ec}\quad T_j = T_{in} + \frac{j}{k}\,(T_s - T_{in});$$

$$\alpha = \alpha_0 \left[\frac{w_{in}}{(w_{in})_0} \right]^{0.8}.$$

2. Temperature of the tube metal in element j [6]:

$$\left(\frac{dT_T}{dt} \right)_{\bar{j}} = \frac{Q_j}{\rho_T c_T (V_T)_j} - \frac{\alpha H_j}{\rho_T c_T (V_T)_j} \left[(T_q)_{\bar{j}} - T_{\bar{j}} \right],$$

$$\left(\frac{dT_q}{dt} \right)_{\bar{j}} = -\frac{Q_j}{0.205\, \rho_T c_T (V_T)_j} + 5.9 \left(\frac{dT_T}{dt} \right)_{\bar{j}} + \frac{(T_T)_{\bar{j}} - (T_q)_{\bar{j}}}{0.205 \tau_i}\,, \tag{2}$$

where τ_i is the internal thermal-delay time [6]. System (2) approximates very closely to the equation of thermal conduction for the perturbation frequencies encountered in boiler operation.

3. The evaporator section in element j:

$$\left(\frac{d\varphi}{dt} \right)_j = \frac{2}{(\rho' - \rho'')\, \Delta z_j} \left\{ [\varphi \rho'' \chi + (1-\varphi)\rho']_j w'_j - [\varphi \rho'' \chi + (1-\varphi)\rho']_{j-1} w'_{j-1} \right\} - \left(\frac{d\varphi}{dt} \right)_{j-1}; \tag{3}$$

with the slip factor

$$\chi_j = \frac{1 - \varphi_j}{\varphi_i}\, \frac{\rho'}{\rho''}\, \frac{X_j}{1 - X_j}\,. \tag{4}$$

The proportion of steam by weight is deduced from the expression for the steam content in terms of pressure as given in [7]:

$$\frac{\beta}{\varphi} = \frac{1}{0.833 + 0.167 X} + \psi(P)\, f(d)\, \mathrm{Fr}_{st}^{-\frac{1}{2}}. \tag{5}$$

From (5) we get

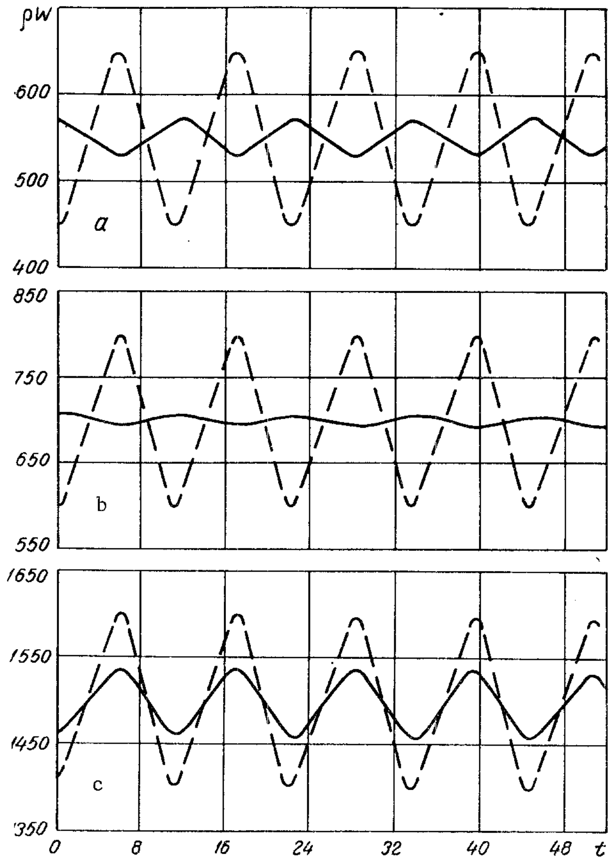

Fig. 3. Time variations in inlet (full line) and outlet (broken line) mass flow rates: a) pulsation state; b) forced inlet flow-rate variations for $\rho\overline{W}$ = 700 kg/m^2·sec; c) the same for $\rho\overline{W}$ = 1500 kg/m^2·sec.

$$X_j = -\frac{0.833v'' + (v' - v'')\varphi_j - 0.167\varphi_j \dfrac{B}{(\rho W)_j}}{0{,}334v''} + \left[\left(\frac{0.833v'' + (v' - v'')\varphi_j - 0.167\varphi_j \dfrac{B}{(\rho W)_j}}{0.334v''}\right)^2 + \frac{v'\varphi_j + 0.833\varphi_j \dfrac{B}{(\rho W)_j}}{0.167v''}\right]^{\frac{1}{2}}, \tag{6}$$

where

$$B = \psi(P) f(d) \left[\frac{d(\rho' - \rho''] g}{\rho''}\right]^{\frac{1}{2}}.$$

Also, ψ(P) and f(d) are functions that take account of the effects of the pressure and tube diameter, which have been derived by processing the abundant experimental evidence. The heat-transfer factor is

$$\alpha_j = [f_1(p)]^{\frac{10}{3}} [(T_q)_{\overline{j}} - T_s]^{\frac{7}{3}}, \tag{7}$$

where

$$f_1(p) = 2.01\,(p^{0.14} + 1.83\cdot 10^{-4} p^2).$$

The speed of the liquid is

$$w'_j = \frac{[A\varphi\chi + A(1-\varphi)]_{j-1} w'_{j-1} + q_j \Delta z_j}{[A\varphi\chi + A(1-\varphi)]_j}, \tag{8}$$

where

$$A = \frac{(i'' - i')\rho'\rho''}{\rho' - \rho''}.$$

The heat flux is

$$q_j = \frac{2}{r_{in}} \alpha_j [(T_q)_{\overline{j}} - T_s]. \tag{9}$$

The density is

$$\rho_j = \varphi\rho'' + (1-\varphi)\rho'. \tag{10}$$

4. The momentum equation

$$\frac{L_c}{g}\frac{d}{dt}(\rho\overline{W}) = \Delta P_c - \sum_{j=0}^{n} (F)_{\overline{j}} \Delta z_j - \frac{1}{g}\sum_{j=0}^{n} \{[\varphi\rho''\chi^2 + (1-\varphi)\rho']_j (w')^2_j - [\varphi\rho''\chi^2 + (1-\varphi)\rho']_{j-1} (w')^2_{j-1}\} + \sum_{j=0}^{n} [\varphi\rho'' + (1-\varphi)\rho']_{\overline{j}} \cos\theta_j \Delta z_j. \tag{11}$$

The speed at the inlet to a tube:

$$= (w_{in})_0 + \Delta w_{in}, \tag{12}$$

$$\Delta w_{in} = \left\{ L_c(\rho\overline{W}) - \rho'(w_{in})_0 (Z_{unh} + Z_{ec}) - \frac{1}{2}\sum_{j=1}^{n} \{[\varphi\rho''\chi + (1-\varphi)\rho']_{j-1} (w'_0)_{j-1} + [\varphi\rho''\chi + (1-\varphi)\rho']_j (w'_0)_j\} \Delta z_j \right\} \times \left\{ \rho'(Z_{unh} + Z_{ec}) + \frac{1}{2}\sum_{j=1}^{n} \{[\varphi\rho''\chi + (1-\varphi)\rho']_{j-1}\sigma_{j-1} + [\varphi\rho''\chi + (1-\varphi)\rho']_j \sigma_j\} \Delta z_j \right\}^{-1}, \tag{13}$$

where

$$(w'_0)_j = \frac{[A\varphi\chi + A(1-\varphi)]_{j-1} (w'_0)_{j-1} + q_j \Delta z_j}{[A\varphi\chi + A(1-\varphi)]_j},$$

$$\sigma_j = \frac{A}{[A\varphi\chi + A(1-\varphi)]}; \qquad \sigma_{j=0} = 1.$$

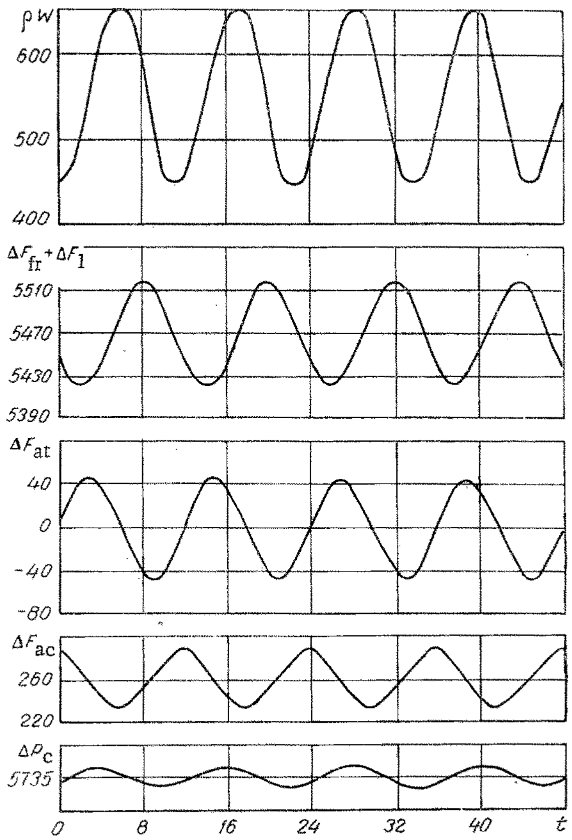

Fig. 4. Time variation in the components of the resistance and in the pressure difference between the collectors during pulsation in a horizontal tube.

The frictional resistance in the single-phase flow:

$$(F_{\mathrm{fr}})_j = \xi_j \frac{(\rho W)_j^2}{2gd\rho_j}, \tag{14}$$

where the coefficient of friction ξ_j is defined [8]

$$\xi_j = 0.0055\{1-0.001[(T_q)_j - T_j]\}\left[1+\left(20\frac{\varepsilon}{d}+\frac{10^6}{\mathrm{Re}_j}\right)^{\frac{1}{3}}\right]. \tag{15}$$

The formula applies for $\mathrm{Re} \geq 4 \times 10^3$. The frictional resistance for the two-phase flow is

$$(F_{\mathrm{fr}})_j = \zeta_j\xi_j \frac{(\rho W)_j^2}{2gd\rho'}\left[1+X_j\left(\frac{\rho'}{\rho''}-1\right)\right], \tag{16}$$

where ζ is the ratio of the coefficients of friction for the actual two-phase flow and for a homogeneous flow, which is defined [9] as a function of Re_j and ρ_j/ρ'. The local resistance is

$$(F_l)_j = \xi_l \frac{(\rho W)_j^2}{2g\rho_j}; \tag{17}$$

$\Delta z_j = 1$ for the local resistance.

Here we give results for the flow pulsations in a set of parallel steam-generating tubes having common inlet and outlet collectors. The pulsations occur in one or more tubes whose thermal or hydraulic conditions are unfavorable, whereas the behavior remains stable in most of the parallel tubes, which have a constant or slightly variable pressure difference between the collectors even when there are pulsations in a tube.

We used an M-220 computer for the numerical integration.

The pulsation model was derived as follows. The pressure difference between the collectors was gradually reduced for a high initial mass flow rate and given initial conditions, which simulates the flow reduction in the shunting system of parallel tubes. The pressure reduction continued until flow-rate pulsations started, after which the pressure difference was kept constant and the pulsations were recorded. At the stability limit, a small reduction in the flow rate caused a considerable increase in the amplitude of the pulsations. If that amplitude was large, the flow rate was markedly nonlinear. The program allowed one to adjust the throttling at the inlet or outlet at any instant, as well as the heat loading and the temperature deficiency at the inlet.

The theoretical solution was compared with tests run on the pulsation test bed at the Polzunov Central Boiler and Turbine Institute [10]. The agreement was good as regards the mean mass flow for pulsation onset and as regards the period of the pulsations (Fig. 1).

Also, direct solution of the equations in partial derivatives made it possible to examine the changes in the principal parameters during the pulsations.

Figure 2 shows the fairly complicated distribution of the flow rate along a tube during the pulsations. The inlet flow rates at definite instants correspond to the curve of Fig. 1b. Figure 2 shows that the pulsations in one part of the tube are opposite in phase to those in the other part, and the point of phase change shifts during a pulsation from the start of the evaporator section to the end.

This instability causes the inlet flow rate to fluctuate in opposite phase to the outlet rate. A stable state was provided by increasing the mean flow rate in a tube. If forced inlet flow-rate variations were produced in the stable state (the amplitude and frequency being similar to those of the pulsations), the variation amplitude in the outlet rate at first fell as the mean flow rate was increased relative to the amplitude of the inlet variation, then became zero, and finally oscillated in phase with the inlet (Fig. 3). This occurred because the evaporation section shortened and there was a reduction in the time to transmit a flow perturbation from the start of that section to the end.

One can deduce the pulsation mechanism from the distribution of the principal parameters in time and along a pipe. If the flow rate falls on account of reduced pressure difference between the collectors, this: 1) increases the length of the evaporation section and also the time to transmit a perturbation along that section, 2) causes increased steam content and hence increases the resistance of the evaporator section. Then (11) for the flow rate in a horizontal tube may be put as

$$\frac{L_c}{g}\ \frac{d}{dt}(\rho\overline{W}) = \Delta P_c - (\Delta F_{fr} + \Delta F_1 + \Delta F_{ac}). \tag{18}$$

If ΔP_c falls, the tube resistance $(\Delta F_{fr} + \Delta F_1 + \Delta F_{ac})$ at first changes only slightly if the length and other quantities are appropriate, and this persists until the flow-rate perturbation has reached the end of the evaporator section. Then (18) shows that the negative quantity of the right side of the equation falls, which increases the rate of reduction in the inlet flow rate. After a certain time, the flow-rate perturbation approaches the end of the tube, where the resistance is greatest, and the right side of (18) starts to increase and becomes positive. Correspondingly, the rate of inlet flow-rate increase from being negative becomes positive, whereas the outlet flow rate continues to fall. If ΔP_c ceases to vary in this period, periodic flow-rate pulsations will persist in the tube, and the resistance components will have certain amplitudes and mutual phase shifts, with the result that the overall tube resistance varies only slightly. Figure 4 shows the pulsations in the resistance components for a horizontal tube. Small pulsations in ΔP_c occur on account of small variations in overall flow rate, but their amplitude settles down at a certain level. If ΔP_c remains constant when the mass flow rate falls to the unstable region, the pulsation amplitude increases as time passes.

This mechanism explains the effects of inlet and outlet throttling. Increase in outlet throttling increases the proportion of the resistance due to the end of a tube, and the length of the evaporation section has to be reduced (i.e., the flow rate has to be increased) if we are to keep unaltered the time for a perturbation to propagate from the start of that section to the part where the resistance changes most rapidly. The stability therefore deteriorates. Inlet throttling shifts the stability limit downwards the most extensively the greater its relative contribution to the total resistance of a tube. In fact, change in inlet flow rate affects the resistance, so the right side of (18) cannot be altered very substantially, and so one has to reduce the flow rate in order to initiate pulsations, which thereby increases the relative contribution of the evaporation section to the total resistance.

NOTATION

ρ	is the density, kg/m^3;
v	is the specific volume, m^3/kg;
c_p	is the specific heat at constant pressure, kcal/kg · deg;
d	is the thermal diffusivity, m^2/h;
λ	is the thermal conductivity, kcal/m · h · deg;
g	is the gravitational acceleration, m/sec^2;
α	is the heat transfer coefficient, kcal/m^2 · hr · deg;
φ, β, X	are the steam contents from pressure, flow, and weight-basis flow;
Q	is the heat, kcal;
T, T_s	are the temperature of medium and saturation, °C;
T_q	is the temperature of tube surface, °C;
T_T	is the mean temperature along tube surface, °C;
q	is the specific heat flux through heat transfer surface per unit length of tube, kcal/m^3 · h;
V	is the volume, m^3;
r_{in}, r_e, d	are the internal and external radii and internal diameter of tube;
L_c	is the length of the tube between collectors, m;
Z_{unh}	is the length of unheated tube at inlet, m;
Z_{ec}	is the length of economizer section, m;
Z	is the length of tube from start, m;
H	is the heat transfer surface, m^2;
Δz	is the step in spatial coordinate, m;
Δt	is the time step, sec;
t	is the time, sec;

w	is the velocity, m/sec;
w_{in}	is the velocity at inlet, m/sec;
Δw_{in}	is the deviation of velocity at inlet from initial value, m/sec;
ρW	is the mass flow rate, $kg/m^2 \cdot sec$;
$\rho \overline{W}$	is the mean mass flow rate in tube, $kg/m^2 \cdot sec$;
χ	is the step factor;
P	is the pressure, kg/cm^2;
θ	is the angle between velocity vector of heat transfer agent and vector of gravitational acceleration, deg;
Re	is the Reynolds number;
Fr_{st}	is the Frud number calculated from the velocity;
ΔP_c	is the pressure drop between collectors, kg/m^2;
F_l	is the equivalent pressure losses in local resistances distributed per unit tube length, kg/m^3;
F_{tr}	is the frictional pressure losses per unit tube length, kg/m^3;
ξ	is the friction drag coefficient;
ζ	is the ratio of resistance coefficients in real and homogeneous two-phase flows;
ξ_l	is the coefficient of local resistance;
ΔF_l	is the total pressure losses in local resistance, kg/m^2;
ΔF_{fr}	is the total pressure losses due to friction, kg/m^2;
ΔF_{ac}	is the pressure loss due to spatial outlet acceleration in tube, kg/m^2;
ΔF_{at}	is the pressure loss due to acceleration with time, kg/m^2.

Subscripts

'	water on saturation line;
"	steam on saturation line;
j	values of parameters at outlet of j-th element;
$\overline{j}$	mean values of parameters on j-th element;
M	parameters referred to tube metal;
0	initial values

LITERATURE CITED

1. S. S. Kutateladze and M. A. Styrikovich, Hydraulics of Gas–Liquid Systems [in Russian], GÉI (1958).
2. Wallis et al., Teploperedacha, 83, series C, No. 3 (1961).
3. Meyer and Rose, Teploperedacha, 85, series C, No. 1 (1963).
4. V. A. Gerliga and I. I. Morozov, Sborn. Trudov ChPI, Izd. Chelyabinsk. Politekh. Inst., 38, 5 (1966).
5. N. Zuber and F. W. Staub, Nuclear Science and Engineering, 30, No. 2 (1967).
6. A. Ya. Kramerov and Ya. V. Shevelev, Engineering Calculation on Nuclear Reactors [in Russian], Atomizdat (1964).
7. Zuber and Findlay, Teploperedacha, 87, series C, No. 4 (1965).
8. Waggener, Nucleonics, 19, No. 11 (1961).
9. S. Levy, Teploperedacha, 85, series C, No. 2 (1963).
10. O. M. Baldina et al., Sb. Trudov VVMIOLU im. Dzerzhinskogo, Leningrad, 66, 37 (1968).
11. A. Nahavandi and R. von Hollen, Nuclear Science and Engineering, 20, No. 4 (1964).
12. W. D. Schultz, Computational Methods in Hydrodynamics [Russian translation], Mir (1967).